J. Phys. Chem. B **1999,** *103,* 7505−7513

Hydrogen Bonding Network Formed between Accumulated Langmuir−Blodgett Films of Barbituric Acid and Triaminotriazine Derivatives

Takeshi Hasegawa,*[,†] Yuko Hatada,[†] Jujiro Nishijo,[†] and Junzo Umemura[‡]

Kobe Pharmaceutical University, Motoyama-kita, Higashinada-ku, Kobe 658-8558, Japan,
and Institute for Chemical Research, Kyoto University, Uji 611-0011, Japan

Qun Huo and Roger M. Leblanc*

Department of Chemistry, University of Miami, P.O. Box 249118, Coral Gables, Florida 33124

Received: April 26, 1999; In Final Form: July 5, 1999

Accumulated Langmuir−Blodgett (LB) films that consist of two layers of barbituric acid (BA) and triaminotriazine (TAZ) derivatives (C_{18}BA and 2C_{18}TAZ) were deposited at various surface pressures on a gold-evaporated glass slide covered with a deuterated cadmium stearate (CdSt-d_{35}) monolayer. The two-monolayer LB films (the CdSt-d_{35} layer is considered to be a part of the substrate) were measured by infrared reflection−absorption (IRRA) spectrometry to investigate the hydrogen-bonding network formed between the two layers. The most notable results were given by the LB film that has the layer configuration of IR//C_{18}BA/2C_{18}TAZ/CdSt-d_{35}/Au. The C_{18}BA layer was deposited at various surface pressures on the 2C_{18}TAZ monolayer. Depending on the surface pressure, the wavenumber of the C═O stretching vibration band (ν(C═O)), derived from BA, showed drastic change. At 20 mN m^{-1}, the C═O groups were found to be in non-hydrogen bonded state (1755 cm^{-1}) to a large extent. The non-hydrogen bonded C═O groups are, in general, rarely seen for the interacted BA/TAZ system. The extraordinary non-hydrogen bonded C═O groups were explained readily by a novel schematic model that was estimated through the molecular orientational analysis. In consequent, the film-to-film interaction is found to give a quite unique hydrogen bonding network structure.

Introduction

Molecular recognition via hydrogen bonding has been noticed from various research fields. Molecular interaction-induced recognition has a large potential to yield important functions in biological systems[1−8] and chemical sensors.[9−14] In fact, many biological molecules are found to have specific molecular recognition properties to present various biological functions.[1−8] In particular, the biological properties of proteins and DNA are mainly governed by the molecular recognition. Reproduction process of DNA by RNA largely depends on the molecular recognition between specific counter-base pairs.[6]

The most understandable driving force to produce the molecular recognition is intermolecular forces. The intermolecular force can be observed by an atomic force microscope (AFM).[15] With the tip of AFM, even one molecule could be manipulated, and the force in pN level between two molecules is observable. Other than the use of AFM, surface force apparatus (SFA)[16] is also known to be a powerful tool to measure the intermolecular force. Kurihara et al.,[17,18] for example, measured the force by SFA to investigate the driving force of the molecular recognition of DNA bases. The interactive force between adenine and thymine (A−T) or T−T was measured as a function of the distance between the bases. The results for the two cases are largely different from each other. The interaction between A−T was always attractive, and the force attains about 200 nm distance. The interaction between T−T, on the other hand, greatly depends on pH of the solution, and the interaction varies from attractive to repulsive. The interactive distance itself also attains about 200 nm.

The results above indicate that the intermolecular force works in long distance through hydrogen bonding. The property, however, also depends on structural fitness between the molecules. Therefore, the structural fitness is the secondary dominant factor of the driving force of the molecular recognition.

In the present study, barbituric acid (BA; Scheme 1a) was chosen to investigate the matter of the structural fitness. BA is one of the most popular neuroactive compounds,[19] because of its highly symmetrical structure and the high potential of hydrogen bonding due to the cyclic imide structure. The unique property of hydrogen bonding of BA has been accepted great interest thus far.[20−26]

The most popular target molecule to BA is triaminotriazine (TAZ; Scheme 1b).[22−26] TAZ is a cyclic amine molecule and interacts with BA very strongly via complementary hydrogen bonding to form supramolecular assemblies. To investigate the property of the two-dimensional molecular assemblies, the Langmuir (L) technique[25] is useful. Kunitake et al.[24] recently synthesized some TAZ derivatives bearing different hydrocarbon chains (tails), and the L films (spread monolayers on water) of these molecules were prepared. Surface pressure (π)−area (A)

---

* To whom correspondence should be sent. Fax: +81 78 441 7541. E-mail: hasegawa@kobepharma-u.ac.jp. FAX: +1 305 284 4571. E-mail: RML@umiami.ir.miami.edu.

[†] Kobe Pharmaceutical University.

[‡] Kyoto University.

10.1021/jp991347v CCC: $18.00

SCHEME 1: Schematic Molecular Structures of C_{18}BA and $2C_{18}$TAZ

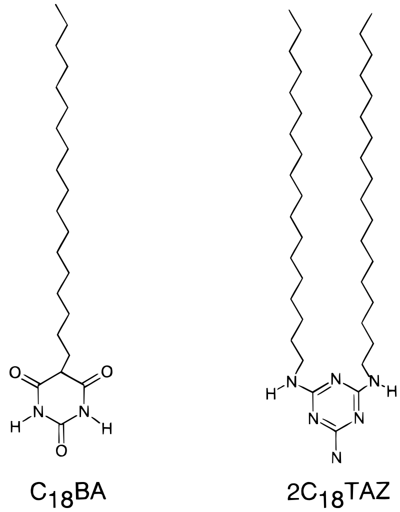

isotherm measurements have been used to investigate the interaction between the TAZ derivative L films and BA from the aqueous subphase. They revealed that the complex formation patterns depend on the molecular cross section area that is defined by the number and conformation of the alkyl tails. For example, the TAZ with four dodecoxyl chains was found to form complementarily a 1:2 complex with BA molecules on water surfaces. Their discussion was supported by infrared reflection−absorption (IRRA) spectrometry[27] of 9- or 10-monolayer Langmuir−Blodgett (LB) films deposited on a gold-evaporated glass slide.

Similar attempts were made by Möbius and Ringsdorf et al.[22−25] Möbius et al.[22] attached a hydrocarbon chain, that includes a chromophore part, to BA molecules, and the prepared L films were stabilized with TAZ molecules dissolved in subphase solution through the molecular recognition at the air−water interface. The hydrolysis reaction of the BA derivatives that depends on the pH of the subphase BA solution was investigated by UV−vis reflection spectrometry at the interface.

Ringsdorf et al.,[25] on the other hand, prepared octadecyl-BA L films on the TAZ aqueous solution, like in the study by Kunitake et al. They investigated the L films as a function of temperature by $\pi-A$ isotherms and infrared external reflection (ER) spectrometry[25,28−30] at the air−water interface (not using LB method). Of particular interest in their study is that the large difference of spectra is due to the substitution position of the octadecyl group on BA. When the octadecyl group is at asymmetric positions, the complex shows unusually high wavenumbers for the carbonyl bands of BA in the ER spectra. When BA is substituted with two octadecyl chains at the symmetric positions, the carbonyl band shifted to a lower wavenumber. Although these results are of great interest, a fine mechanism for the results is not provided.

Recently, Huo et al.[26] have reported the complementary hydrogen bonding mechanism of TAZ and BA with the use of newly synthesized 2-amino-4,6-dioctadecylamino-1,3,5-triazine ($2C_{18}$TAZ). They investigated the surface topography by Brewster angle microscopy[31,32] and the mechanism of autoassembly of the $2C_{18}$TAZ monolayers by UV−vis spectrometry and $\pi-A$ isotherms. They presented in the paper that different complementary hydrogen bonding additives in the subphase solution made different complex formations. With the same method, it was also found that organic solvents diluted in the subphase solution affected the hydrogen bonding network. For example, dimethyl sulfoxide destroys the network, while dioxane enhanced the network formation.

All the above studies are devoted to the investigations of hydrogen bonding networks between "a monolayer and monomers". In the present study, the hydrogen bonding network formation between "two monolayers" of BA and TAZ has been studied by LB and IRRA techniques. For this purpose, dodecyl-BA (C_{18}BA) was synthesized as well as $2C_{18}$TAZ, and two monolayers were laid on each other, which are deposited on a gold-evaporated glass slide by the LB technique. The accumulated monolayers (films) showed specific "film-to-film" interaction that is largely different from "film-to-monomer" or "monomer-to-monomer" interaction. A schematic molecular interaction to explain the specific interaction has been proposed by calculation of the tilt angle of hydrocarbon chains deduced from IRRA spectra.

Experimental Section

Synthesis of C_{18}BA. The synthesis of C_{18}BA has been reported previously.[25] The procedure described here is slightly different from the literature, and the characterization data is also slightly different, as shown below.

Materials. Chemicals for the synthesis were purchased from Aldrich Chemical Co. and used in organic synthesis directly. All organic solvents for the synthesis and purification were purchased from Fisher Scientific Co. as reagent grade and were used without further purification. Thin-layer chromatography (TLC) was conducted on Merck F254 silica gel TLC plates with fluorescent indicator. Flash chromatography was conducted with silica gel (40 μm, particle size 0.041−0.067 mm). The ^{1}H NMR spectra was obtained from a Varian VXR 400 MHz spectrometer. Low-resolution FAB mass spectra were recorded on a VG-Trio 2000 mass spectrometer. Combustion analysis was conducted by Atlantic Microlab Inc. (Norcross, GA).

*Preparation of Diethyl **β**-Octadecylmalonate.* Diethylmalonate (3.20 g, 20 mmol) was added to a ca. 20 mM ethanol containing 20 mmol sodium ethoxide. The reaction mixture was increased to a temperature close to reflux for half an hour. Then, 1-bromooctadecane (6.66 g, 20 mmol) was added very carefully. The resulting mixture was refluxed for 3 h. The reaction mixture was filtered while still hot. The filtrate was concentrated en vacuo, and brown oil liquid product was obtained. The crude product was further purified by flash chromatography with EtOAc/Hexane (1/20, v/v) as the eluent (yield 50%). ^{1}H NMR ($CDCl_3$): δ 4.20 (q, 4H), 3.30 (t, 1H), 1.88 (q, 2H), 1.25 (m, 38H), 0.85 (t, 3H).

Preparation of 5-Octadecylbarbituric Acid (C_{18}BA). To 5 mL of 1.6 M sodium ethoxide, diethyl β-octadecylmalonate (824 mg, 2 mmol) and urea (120 mg, 2 mmol) were added. The reaction mixture was brought to reflux for 9 h, at which point most of the solvent was evaporated out. To the residue, 20 mL water was added and adjusted to pH 6.0 with 6 M HCl. The precipitate was collected by suction filtration and washed with water. The crude product was further purified by recrystallization from EtOH, which yields 50% pure title compound. ^{1}H NMR ($CDCl_3$): δ 7.82 (s, 2H), 3.40 (t, 1H), 2.12 (q, 2H), 1.60−1.15 (m, 32H), 0.83 (t, 3H). FAB MS m/z:(M^++1) calcd for $C_{22}H_{40}N_2O_3$, 380.0; found 381.0. Anal. Calcd for $C_{22}H_{40}N_2O_3$: C, 69.43; H, 10.59; N, 7.36. Found: C, 69.37; H, 10.54; N, 7.36.

Other Materials. $2C_{18}$TAZ was synthesized as previously described in an earlier paper.[26] Both C_{18}BA and $2C_{18}$TAZ were dissolved at 1 mM in mixed solutions of chloroform and methanol (5:1). The organic solvents for the solutions were spectroscopic grade made by Dojindo Laboratories (Kumamoto, Japan). Other organic solvents for cleaning were ethanol, acetone, chloroform, and dichloromethane. They were all extra pure grade and purchased from Wako Pure Chemical Industries Ltd. (Osaka, Japan).

Pure water was obtained through a Millipore Co. (Bedford, MA) Milli-Q Laboratory water purifier with a Millipak 40 filter (0.22 μm pores). The source water for Milli-Q was obtained from a Yamato Scientific Co. Ltd. (Tokyo, Japan) WG-25 autodistiller. The finally obtained pure water showed electric resistance of 18.3 MΩ cm or above.

Gold-evaporated glass slides were provided by Sinyo Co. (Osaka, Japan). The thickness of the gold layer is ca. 300 nm overlaid on a chromium support layer.

Instruments. L film preparations and LB film depositions were performed with a Kyowa Interface Science (Saitama, Japan) model HBM LB film apparatus. The surface pressures were measured by a Wilhelmy balance. The trough size is 14.0 cm (width) × 65.0 cm (length). The solution of C_{18}BA or 2C_{18}-TAZ in 70 μL was dropped by a microsyringe on the water surface in the trough to prepare L films. The compression speed of the monolayer was fixed at 14.0 cm^2 min^{-1} (3.3 $Å^2$ $molecule^{-1}$ min^{-1}). For LB film transfer, the dipping speed was set at 0.5 cm min^{-1} for both LB (vertical dipping) and horizontal lifting (HL)[33] methods. Details about the LB deposition on a substrate will be described in Results and Discussion. Our $\pi-A$ isotherms of the two compounds are almost identical to the previously published isotherms.[25,26] The limited cross section areas of C_{18}BA and 2C_{18}TAZ are 0.36 and 0.48 nm^2 $molecule^{-1}$, respectively.

IRRA measurements were performed on a Nicolet Instrument Co. (Madison, WI) Magna 850 FT-IR spectrometer equipped with a deuterated triglycine sulfate (DTGS) infrared detector at 25 °C. The modulation frequency was fixed at 5 kHz, and the number of scans was 300. The p-polarized infrared ray was obtained with a Hitachi Co. (Ibaragi, Japan) Au/AgBr wire grid polarizer. The reflection measurements were performed with a Harrick Scientific (Ossining, NY) RMA-1DG/VRA variable-angle reflection attachment with retro-mirrors. The angle of incidence of the infrared ray on a sample was 80° from the surface normal.

Theory

Molecular tilt angle was calculated by a procedure proposed by Hasegawa et al.[29] The procedure can take anisotropic optical constants into account. This allows us to take any molecular orientation into account to yield expected absorbance. For fine description, readers refer to the literature.[29] In this section, the outline of the theory is summarized briefly.

The calculation procedure was constructed to calculate absorbance (or reflection−absorbance) of a stratified-monolayers LB film where each layer has finite and constant thickness except for both ends. The absorbance is estimated by calculation of the electric field distribution in the layers where the multiple reflections are assumed. The electric field distribution is governed by the anisotropic complex refractive index in each layer. Since the imaginary part of the complex refractive index (extinction coefficient) directly reflects orientation angle of a transition moment of interest, the anisotropic refractive index was introduced in the calculation procedure.

For various kinds of stratified layers, a matrix equation[29] is commonly used for the calculation. The equations with anisotropic refractive indices are as follows.

$$\tilde{M}_j = \begin{bmatrix} \cos\tilde{\beta}_j & -\dfrac{i}{\tilde{q}_j}\sin\tilde{\beta}_j \\ -i\tilde{q}_j\sin\tilde{\beta}_j & \cos\tilde{\beta}_j \end{bmatrix} \tag{1}$$

$$\tilde{\beta}_j = \frac{2\pi}{\lambda}h_j\frac{\tilde{n}_{jo}}{\tilde{n}_{je}}\tilde{\xi}_j \tag{2}$$

$$\tilde{q}_j = \frac{\tilde{\xi}_j}{\tilde{n}_{jo}\tilde{n}_{je}} \tag{3}$$

$$\tilde{\xi}_j = (\tilde{n}_{je}{}^2 - \tilde{n}_{1o}{}^2\sin^2\theta_1)^{1/2} \tag{4}$$

Here, $\tilde{M}_j$ is a complex characteristic matrix to calculate a matrix that consists of electric and magnetic field vectors, where the subscript j indicates the layer location in the multilayer LB film. The tilde (∼) indicates that a variable under this mark is a complex value. The complex refractive indices in the directions of surface parallel and surface normal are represented by $\tilde{n}_{jo}$ and $\tilde{n}_{je}$, respectively. The thickness of the jth layer is shown by h_j. Infrared radiation of the wavelength of λ was irradiated on the LB film at the angle of incidence of θ_1.

The real part of the refractive index was determined from the literature,[34] and the imaginary part was empirically determined with the use of the value previously confirmed.[29] The determination of the imaginary parts (k_{jo} and k_{je}) is as follows.

$$k_{jo} = k_{jx} = k_{jy} = {}^3/_2 k_{bulk}\sin^2\phi \tag{5}$$

$$k_{je} = k_{jz} = 3k_{bulk}\cos^2\phi \tag{6}$$

With the refractive indices that depend on molecular orientation angle, reflection−absorbance was calculated with the use of eqs 1−4. The orientation angle was determined when the calculated value fitted in with the observed value.

Results and Discussion

2C_{18}TAZ Monolayer LB Film. The monolayers of 2C_{18}-TAZ were deposited by the HL method at various surface pressures (0−30 mN m^{-1}) on a CdSt-d_{35} monolayer which covers a gold-evaporated glass slide (substrate). The CdSt-d_{35} monolayer was prepared at 20 mN m^{-1} for all samples to furnish the surface of the gold substrate hydrophobic. The transfer ratio of the 2C_{18}TAZ monolayer was close to unity. The IRRA spectra of the two-monolayer (IR//2C_{18}-TAZ/CdSt-d_{35}/Au) LB films are shown in Figure 1. For the reference measurement, a gold substrate with no film (IR//Au) was used.

In the higher wavenumber region, it is strikingly shown that all intensities of the C−H stretching vibration bands are comparable with each other. The absolute intensity is very small (see the scale bar). Only at the surface pressure of 5 mN m^{-1}, the bands that arise from the CH_2 stretching vibration modes are a little stronger than those of the CH_3 modes. The asymmetric and symmetric CH_3 stretching vibration bands ($\nu_{as}(CH_3)$ and $\nu_s(CH_3)$) and antisymmetric and symmetric CH_2 stretching vibration bands ($\nu_{as}(CH_2)$ and $\nu_s(CH_2)$) appear at 2964, 2876, 2918, and 2850 cm^{-1}, respectively, for the surface pressures of 15−30 mN m^{-1}. For 5 and 10 mN m^{-1}, the $\nu_{as}(CH_2)$ band appears at 2922 cm^{-1}. A Fermi resonance band,[35] which is comprised of the $\nu_{as}(CH_2)$ band and the overtone of the CH_2 scissoring vibration ($\delta(CH_2)$) band, appears at 2934 cm^{-1}. The resolved Fermi resonance band for 15−25 mN m^{-1} is a little overlaid by the $\nu_{as}(CH_2)$ band, while it is largely overlapped by the strong $\nu_{as}(CH_2)$ band for other surface pressures. These results indicate that the structure of 2C_{18}TAZ monolayers is a

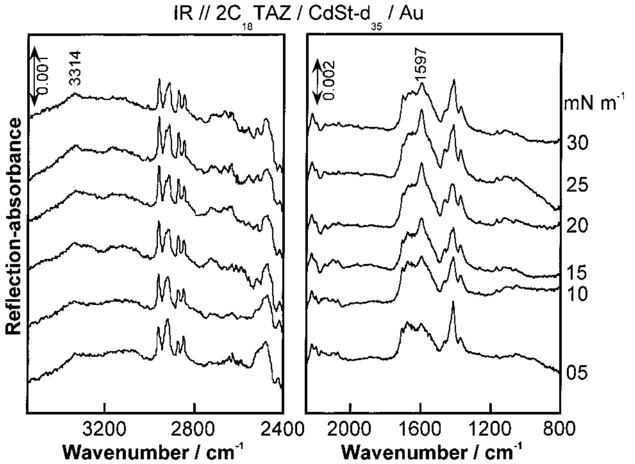

Figure 1. IRRA spectra of $2C_{18}TAZ$ monolayer LB films at various surface pressures deposited on Cd stearate-d_{35} monolayer on a gold-evaporated glass slide.

little disordered when the lateral compression of the monolayers becomes low. Nonetheless, $2C_{18}TAZ$ monolayers are revealed to be quite stable as a whole.

The N−H stretching vibration (ν(N−H)) band is found at 3341 cm^{-1} for all the surface pressures. This wavenumber is specific to the N−H group in amine compounds.[36]

The CH_2 stretching vibration region in Figure 1 shows that the monolayer LB films of $2C_{18}TAZ$ are highly organized. The fact that the $\nu_s(CH_2)$ band stays at 2850 cm^{-1} for all surface pressures indicates that the highly packed monolayer films keep the trans-zigzag molecular conformation well.[37] Judging from the surface selection rule of RA spectrometry,[27,38] the comparable band intensities of the bands in this region strongly indicate that the film molecules ($2C_{18}TAZ$) stand almost perpendicularly to the film surface. IRRA spectra of LB films of metallic salts of stearic acid show, for example, various spectral patterns in the region, which largely depend on counter metallic ions. The most organized LB film we have ever encountered is cadmium stearate LB film.[39] The RA spectrum of cadmium stearate LB film shows quite comparable bands of the C−H stretching vibrations, and the spectral feature is very similar to that of $2C_{18}TAZ$ monolayer LB films. Therefore, the $2C_{18}TAZ$ monolayer is considered to be readily transferred to a gold substrate by the horizontal lifting method.

The tilt angle of the alkyl chain was calculated by the procedure mentioned above, which takes optical anisotropy into account in the calculation. The calculation was carried out for the wavenumber region of 2800−3000 cm^{-1}. The optical constant of the air phase (n_1) is 1.0. The bulk extinction coefficients of the $\nu_{as}(CH_2)$ and $\nu_s(CH_2)$ bands of $2C_{18}TAZ$ (Im($\tilde{n}_{2bulk}$)) are estimated to be 0.362 and 0.274 by taking the number of methylene groups in two alkyl chains of $2C_{18}TAZ$ and the surface area (0.480 nm^2 $molecule^{-1}$) of the molecule into account. The real parts of the refractive indices of the monolayer (Re($\tilde{n}_{2o}$) and Re($\tilde{n}_{2e}$)) were 1.48 and 1.56 for in-plane and out-of-plane components, respectively. The complex refractive indices of the underlayer ($\tilde{n}_{3o}$ and $\tilde{n}_{3e}$) are also 1.48 and 1.56. Since the deuterated compound does not absorb infrared radiation in the wavenumber region, the imaginary parts are zero. The $\tilde{n}_4$ (the gold substrate) is $0.711 + 23.08i$ or $0.738 + 23.58i$ (i = square root of negative one) for the $\nu_{as}(CH_2)$ or $\nu_s(CH_2)$ bands, respectively.[40] The thicknesses of the phases 2 and 3 (h_2 and h_3) are 3.0 and 2.5 nm, respectively. The calculation yielded the tilt angle of the hydrocarbon chain about 5° from the surface normal. The tilt angle may have an analytical error of about 10% due to the error of optical constant estimation. Nonetheless, the analytical error is believed not to affect the discussion significantly. The result supports the above qualitative speculation that the molecules stand almost perpendicularly to the film surface.

In the fingerprint region, the most important band is the band at 1597 cm^{-1} that is derived from the NH_2 bending ($\delta(NH_2)$) mode or the symmetric ring quadrant stretching vibration mode.[41,42] In any case, the transition moment is in the perpendicular direction to the film surface when the molecule stands perpendicularly. This band is most intense when the surface pressure is 15−25 mN m^{-1}. The results also indicate that molecules of $2C_{18}TAZ$ are highly packed, especially at 15−25 mNm^{-1}, and the molecules are oriented perpendicularly to the surface.

When the $\delta(NH_2)$ band increases in intensity, the C−H stretching vibration bands decrease only a little at the same time. Since the direction of transition moment of the $\delta(NH_2)$ band is in the direction of the molecular long axis, the results indicate that the TAZ moiety of the $2C_{18}TAZ$ molecule stands more perpendicularly when the surface pressure is increased, while the hydrocarbon chains do not change largely. Of note is that the hydrocarbon chains are oriented to be almost perpendicular to the film surface even at a low surface pressure.

Since the nitrogen atom in the octadecylamine that covalently attached to the TAZ ring has the sp^2 configuration, it is difficult to have the whole molecule in a plane. In our case, the two alkyl chains are almost parallel to each other and direct to the air phase at the air−water interface at a high surface pressure. Therefore, the molecular plane of the TAZ ring could not have perpendicular orientation even at a high surface pressure. This means that $2C_{18}TAZ$ molecule is believed to have mechanical stress by the high lateral pressure.

In the lower wavenumber region, C−D stretching vibration bands that arise from the underlayer (CdSt-d_{35}) are found in the region of 2050−2250 cm^{-1}. Although the band locations are impervious to the surface pressure, the relative band intensity gradually changes with an increase of the surface pressure, in particular, above 10 mN m^{-1}. These results indicate that the underlayer is highly organized even when the overlayer ($2C_{18}TAZ$) is not highly compressed, while the tilt angle of the underlayer molecules responds to overlayers. This is believed to be because of the molecular stress in the overlayer due to the high surface pressure, although the overlayer itself does not show significant spectral change. This means that the interaction between the layers of CdSt-d_{35} and $2C_{18}TAZ$ is considerably strong.

Another notable band is the symmetric COO^- stretching vibration band ($\nu_s(COO^-)$ at 1412 cm^{-1}) arisen from the underlayer, which accompanies the $\delta(CH_2)$ band centered at 1464 cm^{-1} on the left side. The asymmetric COO^- stretching vibration band ($\nu_{as}(COO^-)$) is weak due to the molecular orientation and the surface selection rule of IRRA spectrometry, and it is hidden in other broad bands. The intensity change of the $\nu_s(COO^-)$ band indicates that the structure of the underlayer is affected by the deposited overlayer ($2C_{18}TAZ$). Prior to the analysis, an attempt was made to remove this band by the subtraction of the reference spectrum (IR//CdSt-d_{35}/Au), but it was not successful. The spectral feature of the CdSt-d_{35} layer in a $2C_{18}TAZ$ LB film was largely different from that on the reference substrate of IR//CdSt-d_{35}/Au. This confirms again that the deposited overlayer had a structural effect on the underlayer. Therefore, the original reference (IR//Au) was chosen for the IRRA analysis in the present study so that the strong $\nu_s(COO^-)$

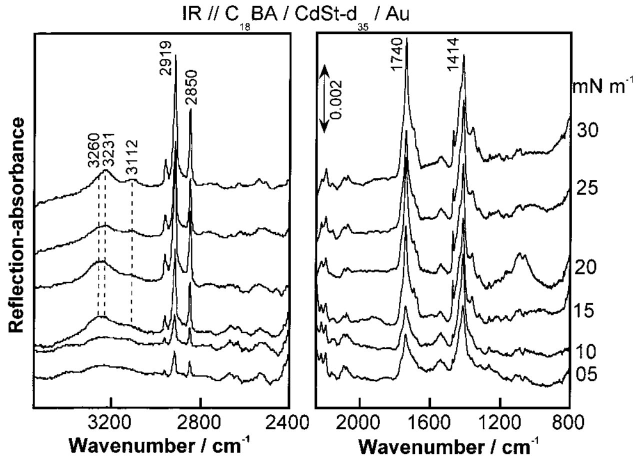

Figure 2. IRRA spectra of $C_{18}BA$ monolayer LB films at various surface pressures deposited on Cd stearate-d_{35} monolayer on a gold-evaporated glass slide.

band and its related bands remain in the spectra. The increase of the $\nu_s(COO^-)$ band is found not to be synchronous with the increase of the C−D stretching vibration bands. This indicates that the motion of the head and tail groups of CdSt-d_{35} are different from each other.

$C_{18}BA$ Monolayer LB Film. $C_{18}BA$ monolayer LB films were prepared on the same substrate in the same manner (IR//$C_{18}BA$/CdSt-d_{35}/Au). In this case, the monolayer transfer by the HL method was not ideally performed. The transfer ratio was almost unity only for the surface pressures of 5 and 10 mN m^{-1}, while it was 1.5 or higher for those above 15 mN m^{-1}. This may indicate that the L film prepared on pure water was partially doubly transferred to the gold substrate at high surface pressures. In the $C_{18}BA$ monolayer deposition, overturning of molecules may have occurred during the HL deposition.

The IRRA spectra of the LB films are shown in Figure 2. It is easily recognized that the surface pressure of 15 mN m^{-1} is a boundary to distinguish the band intensities, especially for bands from $C_{18}BA$ molecules. For example, the C−H stretching vibration bands are very weak for the LB films at 5 and 10 mN m^{-1}, whereas they become abruptly strong for those at 15 mN m^{-1} or higher. An attempt was made to calculate the molecular orientation angles for the bands as described in the previous section, but the extraordinary strong bands were beyond the theoretical values for monolayer LB films at 15 mN m^{-1} or higher. The band intensity change could not be explained by the difference in molecular area of the films either (see refs 25 and 26). Consequently, it was found that $C_{18}BA$ monolayers were, in part, doubly transferred by the HL method at a condensed state.

It is found, in addition, that some high-wavenumber bands (around 3200 cm^{-1}) increase largely in intensity above 15 mN m^{-1}. This also supports that the $C_{18}BA$ L films are partially transferred as an accumulated two-layer film to the gold substrate.

When the surface pressure is low (5 and 10 mN m^{-1}), however, both transfer ratio and RA spectra indicate that the monolayer deposition was readily performed. For example, the C−H stretching vibration bands are weak and the intensities are reasonable for the monolayer. The tilt angle of the hydrocarbon chain was calculated for the loosely packed monolayers.

The extinction coefficients of the $\nu_{as}(CH_2)$ and $\nu_s(CH_2)$ bands are estimated to be 0.208 and 0.158, that take the number of methylene groups in the alkyl chain of $C_{18}BA$ and surface area (0.363 nm^2 molecule^{-1}) of the molecule into account. Other parameters were the same as those mentioned above. The calculated tilt angle of the alkyl chain of $C_{18}BA$ at 5 and 10 mN m^{-1} is about 2.7°. The results indicate that even the loosely packed monolayers are readily transferred to the gold substrate.

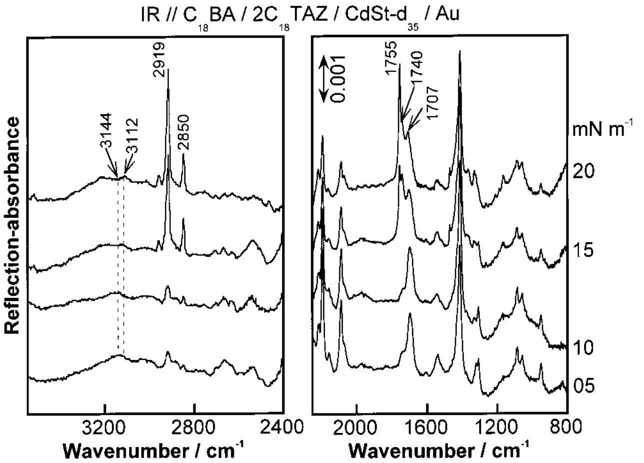

Figure 3. IRRA spectra of accumulated $C_{18}BA/2C_{18}TAZ$ LB films deposited on Cd stearate-d_{35} monolayer on a gold-evaporated glass slide. The $C_{18}BA$ monolayers were prepared at various surface pressures on $2C_{18}TAZ$ monolayer that was prepared at the fixed surface pressure, 20 mN m^{-1}.

At above 15 mN m^{-1}, on the other hand, the $\delta(CH_2)$ band appears clearly at 1470 cm^{-1}. If the $C_{18}BA$ molecule stands perfectly normal to the surface, the transition moment of the $\delta(CH_2)$ band directs parallel to the surface. In other words, the increase of this band indicates that the molecules are getting more tilted as a whole. The increase in intensity of the $\delta(CH_2)$ band, therefore, suggests that the increase of the C−H bands is caused by the tilt of the hydrocarbon chain as well as the extraordinary high transfer ratio. Since the C−H stretching vibration bands stay at fixed positions (2919 and 2850 cm^{-1}), the double layer has trans-zigzag conformation irrespective of surface pressure.

The C−D stretching vibration region indicates that the underlayer is disordered at above 20 mN m^{-1}. This implies that the $C_{18}BA$ monolayer also interacts strongly with the underlayer.

In the fingerprint region, the band at 1740 cm^{-1} abruptly increased in intensity at 15 mN m^{-1} that corresponds well to the results of the C−H stretching vibration bands. This band is attributed to the C═O stretching vibration band derived from dimer BA molecules. This indicates that the $C_{18}BA$ molecules form dimers laterally or between doubly transferred monolayers. The band is also known to be the “Amide I” band[43] that is highly sensitive to hydrogen bonding. The $\delta(CH_2)$ band at 1470 cm^{-1} also drastically increases in intensity at 15 mN m^{-1}.

Accumulated Two-Layer LB Films of $2C_{18}TAZ$ and $C_{18}BA$. Two L films of $2C_{18}TAZ$ and $C_{18}BA$ were deposited to form stratified two-monolayer LB films on a gold substrate covered with CdSt-d_{35} monolayer. The $C_{18}BA$ L films were last transferred to a $2C_{18}TAZ$ monolayer film (IR//$C_{18}BA/2C_{18}TAZ$/CdSt-d_{35}/Au). The $2C_{18}TAZ$ monolayer was prepared at 20 mN m^{-1}. $C_{18}BA$ L films were prepared at various surface pressures (5−20 mN m^{-1}), and laid on the $2C_{18}TAZ$ monolayer by the LB method. The transfer was done well with a transfer ratio of almost unity.

The IRRA spectra of the accumulated LB films are shown in Figure 3. At a low surface pressure (5 and 10 mN m^{-1}) of $C_{18}BA$ monolayer, the C═O stretching vibration (Amide I) band at 1740 cm^{-1} that arises from C_{18}BA (see Figure 2) almost disappears and the strong band at around 1700 cm^{-1} appears instead. This shift of the Amide I band indicates that the C=O group interacts with TAZ moiety through strong hydrogen bonding.[20,23] This is supported by the fact that the bands derived from 2C_{18}TAZ (the band at 1597 cm^{-1}, for example) almost disappear.

At 15 mN m^{-1}, a great change occurs. A new sharp band at 1755 cm^{-1} appears accompanied by the band at 1740 cm^{-1}. When the surface pressure is increased to 20 mN m^{-1}, the band at 1755 cm^{-1} becomes a dominant band in the spectrum. This band is known to be characteristic of carbonyl groups of BA.[20,24] According to Barnes et al.,[20] the band at 1754 cm^{-1} appears when BA molecules are dispersed in an argon matrix. This band shifts to a lower wavenumber, 1694 cm^{-1}, when BA is in the solid state at 20 K due to hydrogen bonding formation. Therefore, the present result strongly indicates that the accumulated layer has free (non-hydrogen bonded) C=O groups at 15 and 20 mN m^{-1}. At 20 mN m^{-1}, in particular, a large amount of free C=O groups proved to be produced. It is striking that the band due to the free C=O groups appear dominantly, although a C_{18}BA monolayer is directly laid on the 2C_{18}TAZ monolayer.

In the high-wavenumber region, the C−H stretching vibration bands also show a dramatic change. These bands arise from alkyl chains in both C_{18}BA and 2C_{18}TAZ monolayers. When the surface pressure is low (5 and 10 mN m^{-1}), the bands are very weak. When the surface pressure is increased to 15 mN m^{-1}, however, the bands increase in intensity drastically. During this large change, the locations of the bands are kept unchanged. The $\nu_{as}(CH_2)$ and $\nu_s(CH_2)$ bands appear at 2919 and 2850 cm^{-1} through all the surface pressures. This means that the alkyl chains are highly organized and the molecular configuration is trans-zigzag. The $\delta(CH_2)$ band (1470 cm^{-1}) appears increasingly at above 15 mN m^{-1}. The strong intensity of this band supports that alkyl chains tilt from the surface normal above 15 mN m^{-1}. This is consistent with the results of the orientational change deduced from the C−H stretching vibration bands.

The weak ν(N−H) band is, on the other hand, found at 3144 cm^{-1} for the LB films at 5 mNm^{-1}, and this band gradually shifts to a lower wavenumber, 3112 cm^{-1}, for the LB film at 20 mN m^{-1}. This band is known to shift to a lower wavenumber when the N−H group is hydrogen bonded. The result, therefore, indicates that the hydrogen bonding through the N−H group becomes stronger with an increase of the surface pressure. This may indicate that the hydrogen bonding distance becomes shorter.

In the lower wavenumber region again, a great change is found in a region of 2050−2250 cm^{-1} that corresponds to the C−D stretching vibration bands. At 5 mN m^{-1}, the $\nu_{as}(CD_2)$ and $\nu_s(CD_2)$ bands (2193 and 2087 cm^{-1}, respectively) are very strong. These band locations indicate that the molecular conformation of the underlayer is highly organized. On closer inspection, the $\nu_{as}(CD_3)$ band is split into two bands at 2219 and 2212 cm^{-1} when the surface pressure of C_{18}BA monolayer is low (unrecognizable in Figure 3). The bands are believed to arise from the $\nu_{as}(CD_3)$ out-of-skeletal and in-skeletal vibration modes, respectively.[44] In general, the $\nu_{as}(CD_3)$ out-of-skeletal vibration band does not appear in RA spectra of LB films, since the transition moment has almost no surface normal component. The appearance of this band as well as the in-skeletal band indicates that the underlayer has tilted alkyl chains with trans conformation at a low surface pressure.

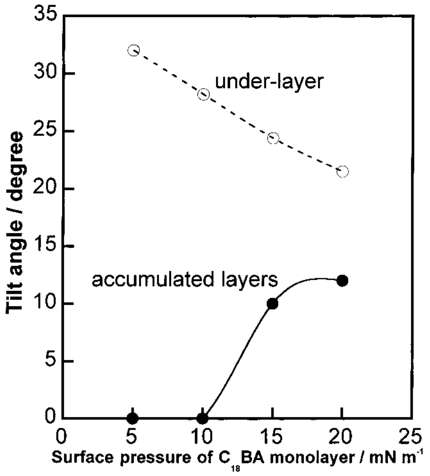

Figure 4. Tilt angle changes of alkyl chains in the accumulated layer and the underlayer shown by solid and dashed lines, respectively.

With an increase of the surface pressure, the $\nu_{as}(CD_2)$ and $\nu_s(CD_2)$ bands decrease in intensity gradually. The band intensity change of the $\nu_s(COO^-)$ mode, however, is not significant, although the band also arises from the same underlayer. This means that the tilt angle of the alkyl chains in the underlayer becomes small by the high surface pressure, but the headgroup is bound to the gold substrate and is stable.

Another important point is that the bands at 1085 and 1093 cm^{-1} appear clearly in all spectra. These bands are assigned to the CD_2 scissoring ($\delta(CD_2)$) mode.[45] The split of this band indicates that the molecular packing of the underlayer is highly organized and the crystal subcell packing is in the orthorhombic form.[46] The bands decrease in intensity with an increase of the surface pressure of C_{18}BA monolayer. As the discussion of the $\delta(CH_2)$ band, the clear appearance of the split bands strongly indicates that the alkyl chains in the underlayer tilt largely, while they are highly organized to have trans conformation.

The tilt angles of the alkyl chain in the accumulated layer and the underlayer as a function of the surface pressure were calculated. The results for the accumulated layer and the underlayer are shown by solid and open circles in Figure 4. The tilt angle of the accumulated layer is almost zero at 5 and 10 mN m^{-1} and jumps up to 10° and 12° from the surface normal at 15 and 20 mN m^{-1}, respectively. The tilt angle of the alkyl chain in the underlayer was, on the other hand, gradually decreased from 32° to 21°. Schematic molecular images are drawn in Figure 5 according to the results in Figure 4.

Parts a and b of Figure 5 are schematic models of the accumulated layer at a low and a high surface pressure of C_{18}BA, respectively. In Figure 5a, the alkyl chains stand almost perpendicularly to the film surface. In the side view, the alkyl chains stand perpendicularly too. The planes of the BA and TAZ rings are a little tilted, in the side view, due to the configuration of the nitrogen atom. Of particular note is that C_{18}BA and 2C_{18}TAZ molecules are complementarily hydrogen bonded and there is no free NH_2 or C=O group. This image is supported by the fact that the C=O stretching bands, found in Figures 1 and 2, are found at around 1700 cm^{-1} (Figure 3).

According to the result in Figure 4, the straight alkyl chain at a high surface pressure tilts 10° or 12° from the surface normal (Figure 5b). At the same time, the alkyl chain in the side view tilts 5.0°. In this case, the coupling mechanism of the C_{18}BA and 2C_{18}TAZ molecules is largely different from that at a low surface pressure. The hydrogen bonding coupling

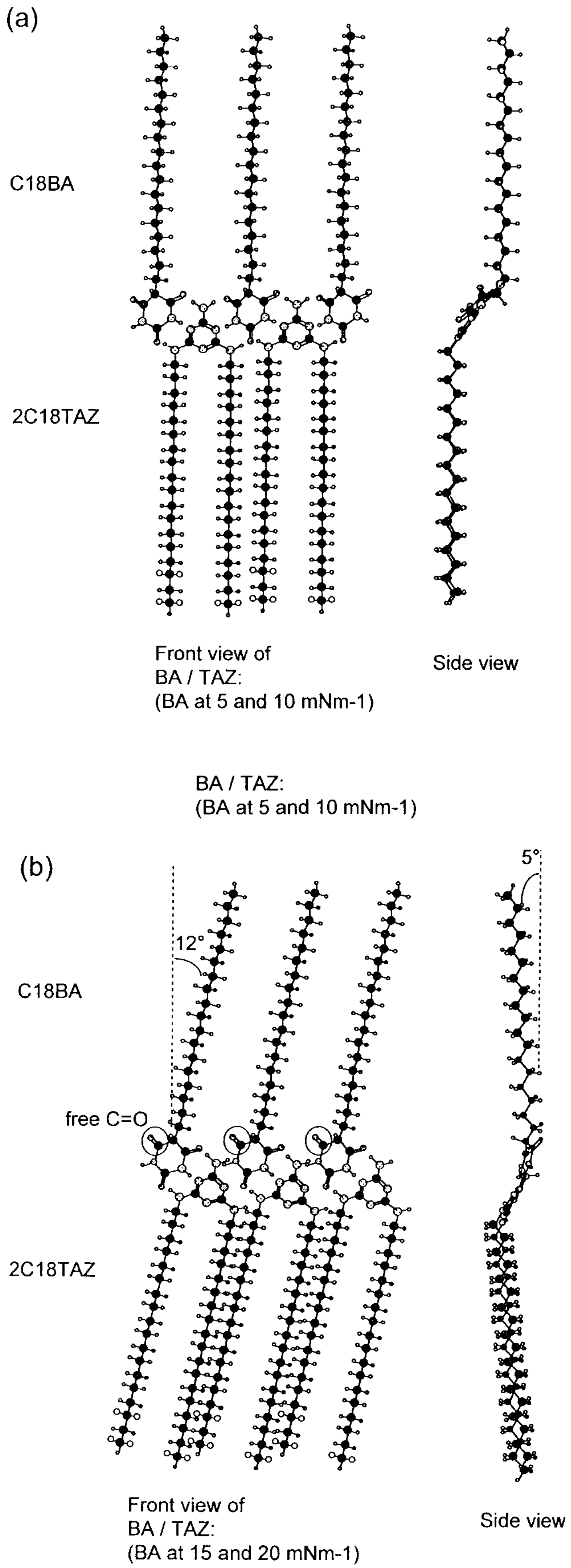

Figure 5. Schematic views of the accumulated layers. The images at (a) low surface pressures and (b) high surface pressures are drawn.

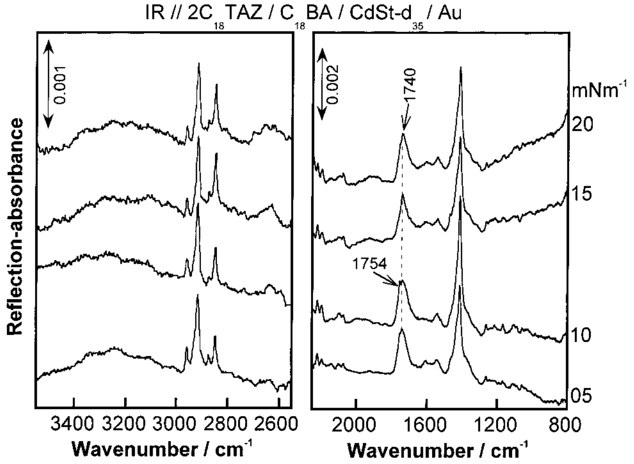

Figure 6. IRRA spectra of accumulated $2C_{18}TAZ/C_{18}BA$ LB films deposited on Cd stearate-d_{35} monolayer on a gold-evaporated glass slide. The $2C_{18}TAZ$ monolayers were prepared at various surface pressures on $C_{18}BA$ monolayer that was prepared at the fixed surface pressure, 20 mN m^{-1}.

is imperfect compared to Figure 5a, and one of the C=O groups in a BA ring remains as a free C=O group. It is possible that the free C=O group does not interact with any groups in the tilted molecule model. This free C=O group is considered to give the free C=O stretching vibration band at 1755 cm^{-1} in Figure 3.

When the surface pressure of $C_{18}BA$ monolayer is high, the molecular density in the monolayer is very high. The highly condensed monolayer is difficult to incorporate into the condensed $2C_{18}TAZ$ monolayer deeply. This means that the film-to-film interaction becomes weak. In this condition, the molecular aggregation by lateral hydrophobic interaction, instead of the interaction between the two layers, should play a dominant role to lead the film to have a close-packed structure. In the close-packed structure, the tilted stance is known to be most stable.[29] Therefore, the molecular tilting stance about 10° with all trans conformation may be reasonable. In other words, the perpendicular molecular stance for the low surface pressures can be considered to be unusual, which must be caused by the extraordinarily strong film-to-film interaction due to the perfect complementary hydrogen bonding.

The orientational change should also affect the orientation of the underlayer. In other words, the gradual orientational change of the underlayer is believed to be a result of the molecular stress in the accumulated layer. The strong stress in the first layer of the LB film was also noted previously in the chain melting process.[29]

In this tilted geometry, the NH_2 group in the TAZ ring is closer to the BA ring compared to the other geometry. This explains the gradual shift of the ν(N−H) band as a function of the surface pressure.

For comparison, the reversed LB layers of the same component films were prepared where $2C_{18}TAZ$ monolayers at various surface pressures were laid on a condensed $C_{18}BA$ monolayer (20 mN m^{-1}). The layer configuration subjected to IRRA measurements is expresses as IR//$2C_{18}TAZ/C_{18}BA$/CdSt-d_{35}/Au.

The IRRA spectra of the LB films are shown in Figure 6. The results are largely different from those for the previous LB films, although the chemical components are the same. It is found that the $C_{18}BA$ monolayer interacts well with the $2C_{18}TAZ$ monolayers regardless of the surface pressure, judging from the loss of the bands that arise from native $2C_{18}TAZ$ (centered at 1597 cm^{-1}). The ν(C=O) band derived from $C_{18}BA$, however, appears at 1740 cm^{-1} with a shoulder or a small peak at 1754 cm^{-1}. The small peak is clearly recognized in the two spectra at low surface pressures (5 and 10 mN m^{-1}). On closer inspection, the intensity of the $\nu_s(CH_2)$ band relatively increases in comparison to the $\nu_a(CH_2)$ band. This suggests that the film molecules are getting tilted in the direction of the side view. In other words, the film molecules show biaxial change with the surface pressure, although the fine chemical mechanism is not clear in this study.

The results indicate that the accumulated layer has an imperfect hydrogen bonding network, since the band at 1707 cm^{-1} is weak. The broad band that is comprised of the bands at 1740 and 1755 cm^{-1} does not change in intensity significantly with an increase of the surface pressure. This must be because the surface area of $C_{18}BA$ is about 25% smaller than that of $2C_{18}TAZ$ at 20 mN m^{-1} (refs 25 and 26). At the small surface area, the molecular packing of $C_{18}BA$ monolayer is highly condensed. The $2C_{18}TAZ$ monolayer is, therefore, difficult to incorporate into the condensed $C_{18}BA$ monolayer deeply. This feature does not depend on the surface pressure of the $2C_{18}$-TAZ monolayer, since the molecular interaction of film-to-film is principally governed by the molecular packing of the $C_{18}BA$ monolayer. Strictly speaking, a very loose $2C_{18}TAZ$ monolayer could interact with the $C_{18}BA$ monolayer, since the film property is a little lost at a very low surface pressure. The split shoulder peak at 1755 cm^{-1}, perceived only for 5 and 10 mN m^{-1}, is consistent with the above speculation.

The C−H stretching vibration region shows no drastic change. One notable point is that the relative intensity of the $\nu_s(CH_2)$ band to the $\nu_{as}(CH_2)$ one increases above 15 mN m^{-1}. This change indicates the biaxial change of the tilt angle of the molecular axis.[47] The result indicates that the molecular plane tilts when the surface pressure is high. The positions of the $\nu_{as}(CH_2)$ and $\nu_s(CH_2)$ bands are 2919 and 2851 cm^{-1}, respectively, and they do not change with the surface pressure.

In the C−D stretching vibration region, the bands that arise from the underlayer do not change at all. The relative intensity of the $\nu_{as}(CD_2)$ band to $\nu_s(CD_2)$ is also stable against the change of surface pressure. The change of $\nu_s(COO^-)$ and $\delta(CH_2)$ bands are not significant. The nonsystematic variance of the band intensity of some bands should be caused by an experimental error.

Molecular Interaction between $2C_{18}TAZ$ LB Film and BA from Aqueous Solution. The above results strongly indicate that the film-to-film interaction responds uniquely to the surface density of the film molecules. To examine the characteristic of the film-to-film interaction, another series of experiment on molecular interaction were performed.

The $2C_{18}TAZ$ monolayers were prepared at 5 and 20 mN m^{-1} on a gold substrate covered with a CdSt-d_{35} monolayer, and the LB films were dipped in a 1 mM BA (without alkyl chains) aqueous solution for 5 and 60 min. After the dipping, they were immediately rinsed by pure water and dried sufficiently in a desiccator. The dried LB films were subjected to IRRA measurements. The RA spectra of the dipped LB films are available in Supporting Information.

The RA spectra of $2C_{18}TAZ$ monolayer LB films at 20 and 5 mN m^{-1} are taken for the same LB film after an equilibration time of 5 and 60 min in the BA solution. All the spectra show a large difference from those of the film-to-film deposited LB films (Figures 3 and 6). Of particular note is that the spectra clearly show a broad band centered at 1597 cm^{-1} where many bands are overlapped with each other. This feature is not found in a spectrum when $2C_{18}TAZ$ reacts well with the BA moiety through hydrogen bonding (Figure 3). The intensity of this band decreases greatly in the spectrum at 5 mN m^{-1}. The change is common for both interaction times. Instead, the band at 1648 or 1705 cm^{-1} increases in intensity relatively.

Although the band at 1648 or 1705 cm^{-1} indicates that the $2C_{18}TAZ$ monolayers partially react with BA molecules, the residual band at 1597 cm^{-1} indicates that the reaction is imperfect for the films at a high surface pressure. Probably, many BA molecules that stack on the $2C_{18}TAZ$ monolayers may cover other nonreacted parts of the monolayer to avoid the perfect reaction.

The same dipping experiment was performed for loosely compressed (5 mN m^{-1}) $2C_{18}TAZ$ monolayers. The spectra of the monolayers are also available in Supporting Information. The intensity of the band at 1597 cm^{-1} largely decreases, and the bands at 1705 and 1648 cm^{-1} increase. These results indicate that the loosely compressed $2C_{18}TAZ$ monolayers bind more BA molecules than the highly compressed monolayers. It is found, however, the film-to-monomer interaction is not so positive compared to the film-to-film interaction.

Conclusion

The film-to-film interaction between the $C_{18}BA$ and $2C_{18}$-TAZ monolayers was revealed to be a unique interaction to produce specific hydrogen bonding networks. When both the two monolayers are highly compressed, molecular interaction between the films becomes weaker due to the imperfect complementary hydrogen bonding formation. In this case, however, the film molecule packing is stabilized by the hydrophobic molecular aggregation force, which results in tilting of film molecules. This process yields many free (non-hydrogen bonded) carbonyl groups. The unique hydrogen bonding network is not recognized between the film-to-monomer interaction. These results indicate that the potential of hydrogen bonding networks of *monolayers* is very strong, which is not found in *monomer* interactions. In other words, two-dimensional molecular assemblies were revealed to have the unique ability of molecular recognition.

Acknowledgment. This work was supported by Grant-in-aid for Scientific Research 09771955 from the Ministry of Education, Science and Culture, Japan to whom the authors' thanks are due.

Supporting Information Available: One figure is available as Supporting Information showing IRRA spectra of $2C_{18}TAZ$ monolayer LB film after dipping in a 1 mM BA aqueous solution. This material is available free of charge via the Internet at http://pubs.acs.org.

References and Notes

(1) Jeong, K.-S.; Tjivikua, T.; Rebek, J., Jr. *J. Am. Chem. Soc.* **1990**, *112*, 3215.

(2) Jacquemain, D.; Leveiller, F.; Weinbach, S. P.; Lahav, M.; Leiserowitz, L.; Kjaer, K.; Als-Nielsen, J. *J. Am. Chem. Soc.* **1991**, *113*, 7684.

(3) Nowick, J. S.; Chen, J. S.; Noronha, G. *J. Am. Chem. Soc.* **1993**, *115*, 7636.

(4) Nowick, J. S.; Chen, J. S.; Noronha, G. *J. Am. Chem. Soc.* **1994**, *116*, 3285.

(5) Kielkopf, C. L.; White, S.; Szewczyk, J. W.; Turner, J. M.; Baird, E. E.; Dervan, P. B.; Rees, D. C. *Science* **1998**, *282*, 111.

(6) Franklin, S. J.; Barton, J. K. *Biochemistry* **1998**, *37*, 16093.

(7) Owen, D. J.; Evans, P. R. *Science* **1998**, *282*, 1327.

(8) Woods, R. J.; Pathiaseril, A.; Wormald, M. R.; Edge, C. J.; Dwek, R. A. *Eur. J. Biochem.* **1998**, *258*, 372.

(9) Bousse, L.; McReynolds, R. J.; Kirk, G.; Dawes, T.; Lam, P.; Bemiss, W. R.; Parce, J. W. *Sens. Actuators, B: Chem.* **1994**, *B20*, 145.

(10) Gopel, W.; Schierbaum, K. D. W. *Sens. Actuators, B: Chem.* **1995**, *B26*, 1.

(11) Kurosawa, S.; Arimura, T.; Tamura, M.; Shibakami, M.; Sekiya, A.; Kamo, N. *Jpn. J. Appl. Phys. 1* **1995**, *34*, 3658.

(12) Piletsky, S. A.; Pietskaya, E. V.; Elgersma, A. V.; Yano, K.; Karube, I.; Parhometz, Yu. P.; Elskaya, A. V. *Biosens. Bioelectron.* **1995**, *10*, 959.

(13) Rickert, J.; Weiss, T.; Gopel, W. *Sens. Actuators, B: Chem.* **1995**, *B31*, 45.

(14) Pizziconi, V. B.; Page, D. L. *Biosens. Bioelectron.* **1997**, *12*, 287.

(15) Rief, M.; Gautel, M.; Oesterhelt, F.; Fernandez, J. M.; Gaub, H. E. *Science* **1997**, *276*, 1109.

(16) Israelachivili, J. N. *Intermolecular and Surface Forces*, 2nd ed.; Academic Press: London, 1991.

(17) Berndt, P.; Kurihara, K.; Kunitake, T. *Langmuir* **1995**, *11*, 3083.

(18) Kurihara, K.; Abe, T.; Nakashima, N. *Langmuir* **1996**, *12*,.

(19) Pearce, R. J.; Duchen, M. R. *J. Physiol.* **1995**, *483*, 407.

(20) Barnes, A. J.; Le Gall, L.; Lauransan, J. *J. Mol. Struct.* **1979**, *56*, 15.

(21) Scoponi, M.; Polo, E.; Pradella, F.; Bertolasi, V.; Carassiti, V.; Goberti, P. *J. Chem. Soc., Perkin Trans. 2* **1992**, 1127.

(22) Ahuja, R.; Caruso, P.-L.; Möbius, D.; Paulus, W.; Ringsdorf, H.; Wildburg, G. *Angew. Chem., Int. Ed. Engl.* **1993**, *32*, 1033.

(23) Bohanon, T.; Denzinger, S.; Fink, R.; Paulus, W.; Ringsdorf, H.; Weck, M. *Angew. Chem., Int. Ed. Engl.* **1995**, *34*, 58.

(24) Koyano, H.; Bissel, P.; Yoshihara, K.; Ariga, K.; Kunitake, T. *Chem.—Eur. J.* **1997**, *3*, 1077.

(25) Weck, M.; Fink, R.; Ringsdorf, H. *Langmuir* **1997**, *13*, 3515.

(26) Huo, Q.; Russel, K. C.; Leblanc, R. M. *Langmuir* **1998**, *14*, 2174.

(27) Takenaka, T.; Umemura, J. *Vibrational Spectra and Structure Vol. 19*; Durig, J. R., Ed.; Elsevier Science: Amsterdam, 1991; p 215.

(28) Dluhy, R. A.; Cornell, D. G. *J. Phys. Chem.* **1985**, *89*, 3195.

(29) Hasegawa, T.; Takeda, S.; Kawaguchi, A.; Umemura, J. *Langmuir* **1995**, *11*, 1236.

(30) Sakai, H.; Umemura, J. *Langmuir* **1998**, *14*, 6249.

(31) Kato, T.; Tatehana, A.; Suzuki, N.; Iimura, K.; Araki, T.; Iriyama, K. *Jpn. J. Appl. Phys.* **1995**, *34*, L911.

(32) Iimura, K.; Suzuki, N.; Kato, T. *Bull. Chem. Soc. Jpn.* **1996**, *69*, 1201.

(33) Iwahashi, M.; Naito, F.; Watanabe, N.; Seimiya, T. *Chem. Lett.* **1985**, *1985* 187.

(34) Paudler, M.; Ruths, J.; Riegler, H. *Langmuir* **1992**, *8*, 184.

(35) Umemura, J.; Mantsch, H. H.; Cameron, D. G. *J. Colloid Interface Sci.* **1981**, *83*, 558.

(36) Colthup, N. B.; Daly, L. H.; Wiberley, S. E. *Introduction to Infrared and Raman Spectroscopy*, 3rd ed.; Academic Press: London, 1990.

(37) Senak, L.; Moore, D.; Mendelsohn, A. *J. Phys. Chem.* **1995**, *96*, 2749.

(38) Greenler, R. G. *J. Chem. Phys.* **1966**, *44*, 310.

(39) Hasegawa, T.; Kamata, T.; Umemura, J.; Takenaka, T. *Chem. Lett.* **1990**, 1543.

(40) Ordal, M. A.; Long, L. L.; Bell, R. J.; Bell, S. E.; Bell, R. R.; Alexander, R. W., Jr.; Ward, C. A. *Appl. Opt.* **1983**, *22*, 1099.

(41) Wang, Y. L.; Mebel, A. M.; Wu, C. J.; Chen, Y. T.; Lin, C. E.; Jiang, J. C. *J. Chem. Soc., Faraday Trans.* **1997**, *93*, 3445.

(42) Scoponi, M.; Polo, E.; Pradella, F.; Bertolasi, V.; Carassiti, V.; Goberti, P. *J. Chem. Soc., Faraday Trans.* **1992**, *2*, 1127.

(43) Crowe, J. H.; Crowe, L. M.; Carpenter, J. F.; Rudolph, A. S.; Wistrom, C. A.; Sparge, B. J.; Anchordoguy, T. J. *Biochim. Biophys. Acta* **1988**, *947*, 367.

(44) Snyder, R. G.; Hsu, S. L.; Krimm, S. *Spectrochim. Acta* **1978**, *465*, 260.

(45) Snyder, R. G. *J. Mol. Struct.* **1961**, *7*, 116.

(46) Malta, V.; Celotti, G.; Zannetti, R. *J. Chem. Soc.* **1971**, *B1971*, 548.

(47) Nakagoshi, A.; Wang, Y.; Ozaki, Y.; Iriyama, K. *Langmuir* **1995**, *11*, 3610.